J. Am. Soc. Mass Spectrom. (2018) 29:2227–2236
DOI: 10.1007/s13361-018-2030-y

RESEARCH ARTICLE

3-Hydroxy-2-Nitrobenzoic Acid as a MALDI Matrix for In-Source Decay and Evaluation of the Isomers

Yuko Fukuyama,[1] Shunsuke Izumi,[2] Koichi Tanaka[1]

[1]Koichi Tanaka Mass Spectrometry Research Laboratory, Shimadzu Corporation, 1, Nishinokyo Kuwabara-cho, Nakagyo-ku, Kyoto, 604-8511, Japan
[2]Department of Mathematical and Life Sciences, Graduate School of Science, Hiroshima University, 1-3-1 Kagamiyama, Higashi-Hiroshima, 739-8526, Japan

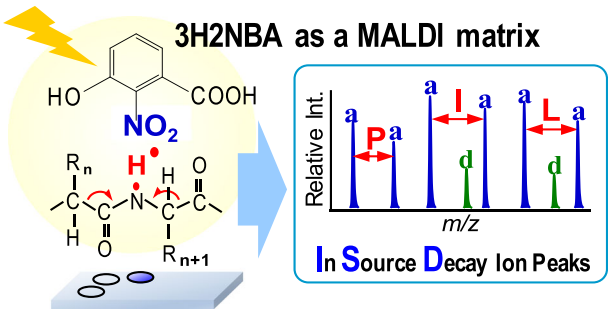

Abstract. In in-source decay (ISD) in matrix-assisted laser desorption/ionization (MALDI)-mass spectrometry (MS), 1,5-diaminonaphthalene (1,5-DAN) is a most frequently used matrix probably due to the highly sensitive detection of fragment ions. 1,5-DAN is a reducing matrix generating *c*- and *z*-series ions by N–Cα bond cleavage. However, it is difficult for reducing matrices to distinguish leucine and isoleucine, and generate $c_{(n-1)}$-series ions owing to proline (Pro) at residues *n*. Oxidizing matrices providing *a*- and *x*-series ions accompanied by *d*-series ions by Cα–C bond cleavage solve the problem, but their sensitivity of the ISD fragment ions has been lower than reducing matrices such as 1,5-DAN. Recently, 3-hydroxy-4-nitrobenzoic acid (3H4NBA) had been reported as an oxidizing matrix generating *a*-series ions with higher intensity compared with conventional oxidizing matrices such as 5-nitrosalicylic acid, but a little lower intensity compared with 1,5-DAN (Anal Chem 88, 8058–8063, 2016). In this study, 3H4NBA isomers (2H3NBA, 2H4NBA, 2H5NBA, 2H6NBA, 3H2NBA, 3H5NBA, 4H2NBA, 4H3NBA, 5H2NBA, and 3H4NBA) were evaluated. All the isomers generated *a*-series ions accompanied by *d*-series ions, wherein 3H2NBA, 3H5NBA, 4H2NBA, 4H3NBA, and 5H2NBA were first confirmed as oxidizing matrices for ISD. Among the isomers, 3H2NBA and 4H3NBA generated *a*-series ions with higher peak intensity compared with 3H4NBA for several peptides. Especially, 3H2NBA generated *a*-series ions with almost the same or higher intensity, and clearly higher peak resolution compared with *c*-series ions using 1,5-DAN in several cases. 3H2NBA was expected to contribute to ISD analyses in MALDI-MS as one of the most effective oxidizing matrices.

Keywords: ISD, MALDI-MS, Matrix, Cα–C bond cleavage

Received: 10 May 2018/Revised: 26 June 2018/Accepted: 6 July 2018/Published Online: 30 July 2018

Introduction

Matrix-assisted laser desorption/ionization (MALDI) [1–4] and electrospray ionization (ESI) mass spectrometry (MS) [5] have been used for the rapid peptides and proteins analyses. In MALDI, collision-induced dissociation (CID) [6], post-source decay (PSD) [7], and in-source decay (ISD) [8, 9] have been used for fragmentation. Among them, ISD enables rapid peptide sequencing by detecting *c*- and *z*-series ions, or *a*- and *x*-series ions with *d*-series ions. In addition, ISD is theoretically unlimited in mass, and thus useful for peptides and also proteins [10]. However, the effect of ISD depends on the matrices [11].

ISD matrices are classified into the following two groups: (1) a reducing matrix which yields *c*- and *z*-series ions by N–Cα bond cleavage, and (2) an oxidizing matrix which yields *a*- and *x*-series ions accompanied by *d*-series ions by Cα–C bond cleavage. The former includes 1,5-diaminonaphthalene (1,5-DAN) [10], 2,5-dihydroxybenzoic acid (2,5-DHB) [12–16], 5-aminosalicylic acid (5-ASA) [17], 5-amino-1-naphthol (5,1-

Electronic supplementary material The online version of this article (https://doi.org/10.1007/s13361-018-2030-y) contains supplementary material, which is available to authorized users.

Correspondence to: Yuko Fukuyama; *e-mail:* yukof@shimadzu.co.jp

ANL) [18], 1,5-dihydroxylnaphthalene (1,5-DHN) [18], 2-aminobenzoic acid (2-AA) [19], and 2-aminobenzamide (2-AB) [19]. The latter includes 5-nitrosalicylic acid (5-NSA, 2H5NBA) [20, 21], 5-formylsalicylic acid (5-FSA) [20, 21], 4-nitrosalicylic acid (4-NSA, 2H4NBA) [21], 3-nitrosalicylic acid (3-NSA, 2H3NBA) [21], or 2,5-bis(2-hydroxyethoxy)-7,7,8,8-tetracyanoquinodimethane (bisHE-TCNQ) [22]. 5-FSA was reported to yield both *c*- and *z*-series ions by N–Cα bond cleavage and *a*- and *x*-series ions by Cα–C bond cleavage. 1,5-DAN and 2,5-DHB as reducing matrices and 5-NSA and bisHE-TCNQ as oxidizing matrices have been reported as higher sensitivity than others in each group [10, 22–24]. In total, 1,5-DAN has been most frequently used for ISD [10, 23, 24], probably due to the highly sensitive detection of fragment ions [10, 25–29].

There are some issues for 1,5-DAN as a reducing matrix as follows: (i) The $c_{(n-1)}$-series ions lack owing to proline (Pro) at residues *n* [16]. (ii) It is difficult to distinguish leucine (Leu) and isoleucine (Ile) having the same mass but a different structure. Oxidizing matrices solve the problems (i)–(ii), but the sensitivity of the fragment ions has been lower than reducing matrices such as 1,5-DAN. (iii) Inhomogeneous matrix/analyte dried spot is formed using 1,5-DAN, which leads to lower peak resolution and reproducibility. (iv) Sublimation property of 1,5-DAN causes lower reproducibility and limits long-time measurement. (v) Lower stability in solution for 1,5-DAN based on oxidation leads to reducing the sensitivity. (vi) In addition, 1,5-DAN has been reported for carcinogenic property [30].

In previous report, 3-hydroxy-4-nitrobenzoic acid (3H4NBA) was introduced as an oxidizing matrix for ISD [31]. It provides *a*- and *x*-series ions accompanied by *d*-series ions by Cα–C bond cleavage with higher sensitivity compared with conventional oxidizing matrices such as 5-NSA (2H5NBA). The sensitivity of ISD fragment ions was a little lower compared with 1,5-DAN. The matrix/analyte dried spot was thin and almost homogeneous, and thus achieved higher mass resolution compared with 1,5-DAN. Toxicity has not been reported, and the slow sublimation and high stability in solution were confirmed. Therefore, 3H4NBA solved all the issues (i)–(vi) of 1,5-DAN. A little lower sensitivity of ISD fragment ions has been remained as only an issue of 3H4NBA compared with 1,5-DAN.

In this study, 3H4NBA isomers (hydroxynitrobenzoic acids) [2-hydroxy-3-nitrobenzoic acid (2H3NBA), 2-hydroxy-4-nitrobenzoic acid (2H4NBA), 2-hydroxy-5-nitrobenzoic acid (2H5NBA), 2-hydroxy-6-nitrobenzoic acid (2H6NBA), 3-hydroxy-2-nitrobenzoic acid (3H2NBA), 3-hydroxy-5-nitrobenzoic acid (3H5NBA), 4-hydroxy-2-nitrobenzoic acid (4H2NBA), 4-hydroxy-3-nitrobenzoic acid (4H3NBA), 5-hydroxy-2-nitrobenzoic acid (5H2NBA), and 3H4NBA] were evaluated as oxidizing matrices for ISD to improve the sensitivity of the fragment ions. Among them, 2H3NBA, 2H4NBA, and 2H5NBA had been reported by Asakawa et al. [11, 20–23]. The other isomers except 3H4NBA are first evaluated. The isomers were also compared with 1,5-DAN. Peak intensity and peak resolution for the ISD fragment ions, and other characteristic feature are discussed below.

Experimental

Materials

2H3NBA, 2H4NBA, 2H5NBA, 3H2NBA (Figure 1Aa), 5H2NBA (Figure 1Aa), and 1,5-DAN (Figure 1Ab) were purchased from Tokyo Chemical Industry Co., Ltd. (Tokyo, Japan). 2H6NBA and 4H2NBA (Figure 1Aa) were purchased from Ark Pharm, Inc. (IL, USA). 4H3NBA (Figure 1Aa) and 3H4NBA (Figure 1Ab) were synthesized by ourselves, but these are also commercially available. Amyloid β 1–16 and amyloid β 1–40 were purchased from Peptide Institute, Inc. (Osaka, Japan). 3H5NBA (Figure 1Aa), *N*-acetyl renin substrate, angiotensin I, and adrenocorticotropic hormone fragment 18–39 (ACTH 18–39) were purchased from Sigma-Aldrich Corp. (St. Louis, MO, USA). 3,4-Dinitrobenzoic acid (3,4-DNBA) and acetonitrile (CH_3CN) (LC/MS grade) was purchased from Wako Pure Chemical Industries, Ltd. (Osaka, Japan). Water used in all experiments was deionized using a *Milli-Q* ultrapure water purification system (Merck Ltd., Tokyo, Japan). All other chemicals were of analytical reagent grade.

Preparation

N-Acetyl renin substrate was dissolved in water at 20 pmol/μL. Angiotensin I, amyloid β 1–16, amyloid β 1–40, and ACTH 18–39 were dissolved in CH_3CN/H_2O/TFA (50:50:0.1, *v*/*v*) at 20 pmol/μL. The matrix solution was prepared in CH_3CN/H_2O (75:25, *v*/*v*) at 10 mg/mL. The analyte solution (0.5 μL) and the matrix solution (0.5 μL) were mixed on a stainless-steel plate (sample plate 2.8 mm ring × 384 well, Shimadzu/Kratos, UK) for analyses using a MALDI time-of-flight mass spectrometer (TOFMS).

MALDI-MS

MALDI TOFMS measurement was performed using an *AXIMA Performance* (Shimadzu/Kratos, UK) mass spectrometer equipped with a nitrogen UV laser (337 nm) in linear positive-ion mode. Data was obtained using raster scanning with five shots of laser irradiation at each of the 1600 data points (at 40 × 40 lattice) in square regions of 1200 μm × 1200 μm~1700 μm × 1700 μm inside a matrix/analyte crystal spot. All the mass spectra were obtained by using almost the same laser power.

Results and Discussion

Evaluation of 3H4NBA Isomers

3H4NBA isomers (2H3NBA, 2H4NBA, 2H5NBA, 2H6NBA, 3H2NBA, 3H5NBA, 4H2NBA, 4H3NBA, 5H2NBA, and 3H4NBA) were evaluated as matrices for ISD. A lot of *a*-

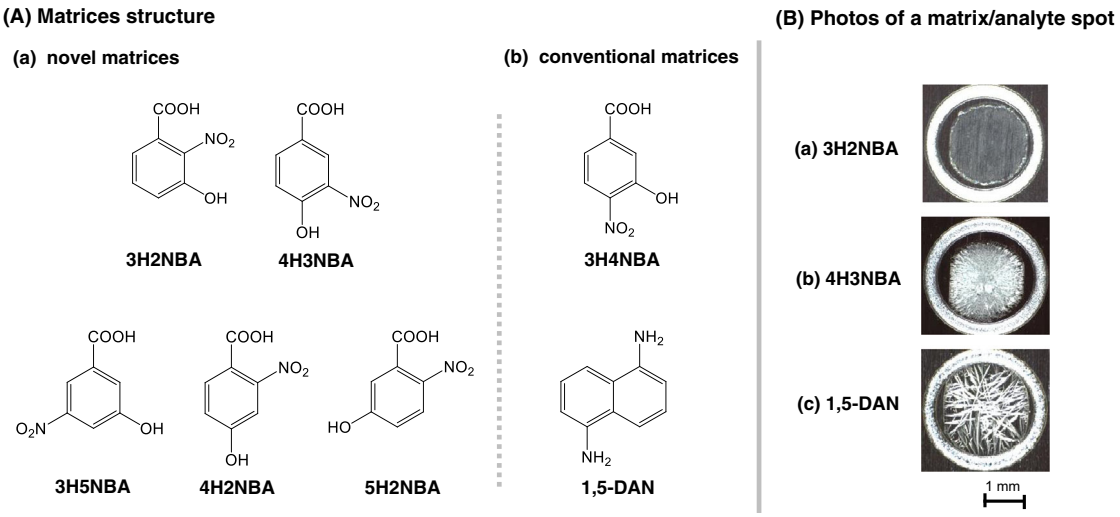

Figure 1. (**A**) Matrices structure of (**a**) 3-hydroxy-2-nitrobenzoic acid (3H2NBA) and the isomers (4H3NBA, 3H5NBA, 4H2NBA, and 5H2NBA) as novel oxidizing matrices for ISD, and (**b**) 3H4NBA as an oxidizing matrix reported before and 1,5-diaminonaphthalene (1,5-DAN) as a conventional reducing matrix for ISD, and (**B**) photos of a matrix/analyte dried spot on a MALDI sample plate using (**a**) 3H2NBA, (**b**) 4H3NBA, and (**c**) 1,5-DAN as matrices

and *d*-series ions were detected using all the isomers. In comparison between 2H3NBA, 2H4NBA, 2H5NBA, 2H6NBA, and 3H4NBA, *a*- and *d*-series ions were detected with higher sensitivity using 3H4NBA than the others (data not shown), which correspond to the previous report [31]. Subsequently, the other isomers (3H2NBA, 3H5NBA, 4H2NBA, 4H3NBA, and 5H2NBA) and 3H4NBA were evaluated.

Figure 2 presents ISD spectra of *N*-acetyl renin substrate using 3H2NBA, 4H3NBA, 5H2NBA, 3H5NBA, 4H2NBA, 3H4NBA, and 1,5-DAN as matrices. Intensity, S/N ratio, and resolution of the representative ion peak (a_{10}- and c_{10}-ion peaks), and intensity of the precursor ion ($[M+H]^+$) and the d_{10}-ion are also indicated. Overall view of the spectra in Figure 2 is shown in Supplemental Information (Figure S1). The *a*- and *d*-series ions were detected using all the isomers. Herein, 3H2NBA, 4H3NBA, 5H2NBA, 3H5NBA, and 4H2NBA were first confirmed as oxidizing matrices for ISD. The mechanism for the formation of *d*-series ions from *a*-series ions has been reported by Asakawa et al. [20, 22]. Generally, *d*-series ions provide structure information for side chains of amino acids, and thus *d*-series ions effectively distinguish Leu from Ile wherein Leu and Ile have the same mass but a different structure. Thus, the *a*-series ions were more useful for obtaining peptide sequence information compared with *c*-series ions. In addition, the $c_{(n-1)}$-series ions lack owing to Pro at residues *n* [16]. In Figure 2 and S1, the a_6-ion was detected even at the N-terminal side of Pro, and the two Leu and one Ile were distinguished by the d_5-, d_{10}-, and d_{11}-ions using the isomers (Figure 2a–f and Figure S1a–f). However, this sequencing is difficult to achieve for *c*-series ions using 1,5-DAN (Figure 2g and Figure S1g). In Fact, the c_6-ion was not detected using 1,5-DAN (Figure S1g).

Comparison of 3H2NBA, 4H3NBA, 5H2NBA, 3H5NBA, and 4H2NBA with 3H4NBA indicated that peak intensity of *a*-series ions was improved using 3H2NBA or 4H3NBA compared with 3H4NBA (Figure 2a–f). In this case, the peak intensity increased about 2-fold using 3H2NBA compared with 4H3NBA (Figure 2a, b) and about 20-fold compared with 3H4NBA (Figure 2a, f). 3H2NBA generated *a*-series ions with highest peak intensity among the isomers. In addition, the peak intensity of *a*-series ions by 3H2NBA increased a few-fold compared with *c*-series ions by 1,5-DAN (Figure 2a, g). S/N ratio was almost the same using 3H2NBA compared with 1,5-DAN (Figure 2a, g). Peak resolution of the *a*-series ions using 3H2NBA was clearly higher than that of *c*-series ions using 1,5-DAN (Figure 2a, g). These results indicate that 3H2NBA as an oxidizing matrix improved peak intensity and peak resolution of ISD fragment ions compared with not only 3H4NBA as a previously reported oxidizing matrix [31] but also 1,5-DAN as a most frequently used reducing matrix [10, 23–29]. It is to be noted that *a*- and *c*-series ions were respectively detected in a little different *m/z* area and from a different fragmentation mechanism. Thus, stringent comparison is impossible for both series ions even though these data are obtained with the same laser power. Nevertheless, ISD spectra were unambiguously high quality using 3H2NBA compared with other matrices including 1,5-DAN.

All the 3H2NBA and the isomers absorbed UV laser (337 nm) and the absorption maximum of them were nearby 337 nm (data not shown). The absorbance at 337 nm was higher in the following order: (4H2NBA, 3H2NBA) < 2H6NBA < (3H5NBA, 4H3NBA, 2H4NBA, 3H4NBA, 2H3NBA) < (5H2NBA, 2H5NBA) < 1,5-DAN. The order of the absorbance correlates poorly with the intensity of *a*-series ions in Figure 2.

In Figure 2, peak intensity of the precursor ion ($[M+H]^+$) was higher using 3H2NBA or 4H3NBA compared with 3H4NBA or 1,5-DAN. In addition, relative ratio of *a*-series ions (or *c*-series ions) for the precursor ion, that is, *a*-series ions yield from the precursor ion, was higher in the following order: 4H2NBA < 3H4NBA < 5H2NBA < 3H5NBA < 4H3NBA

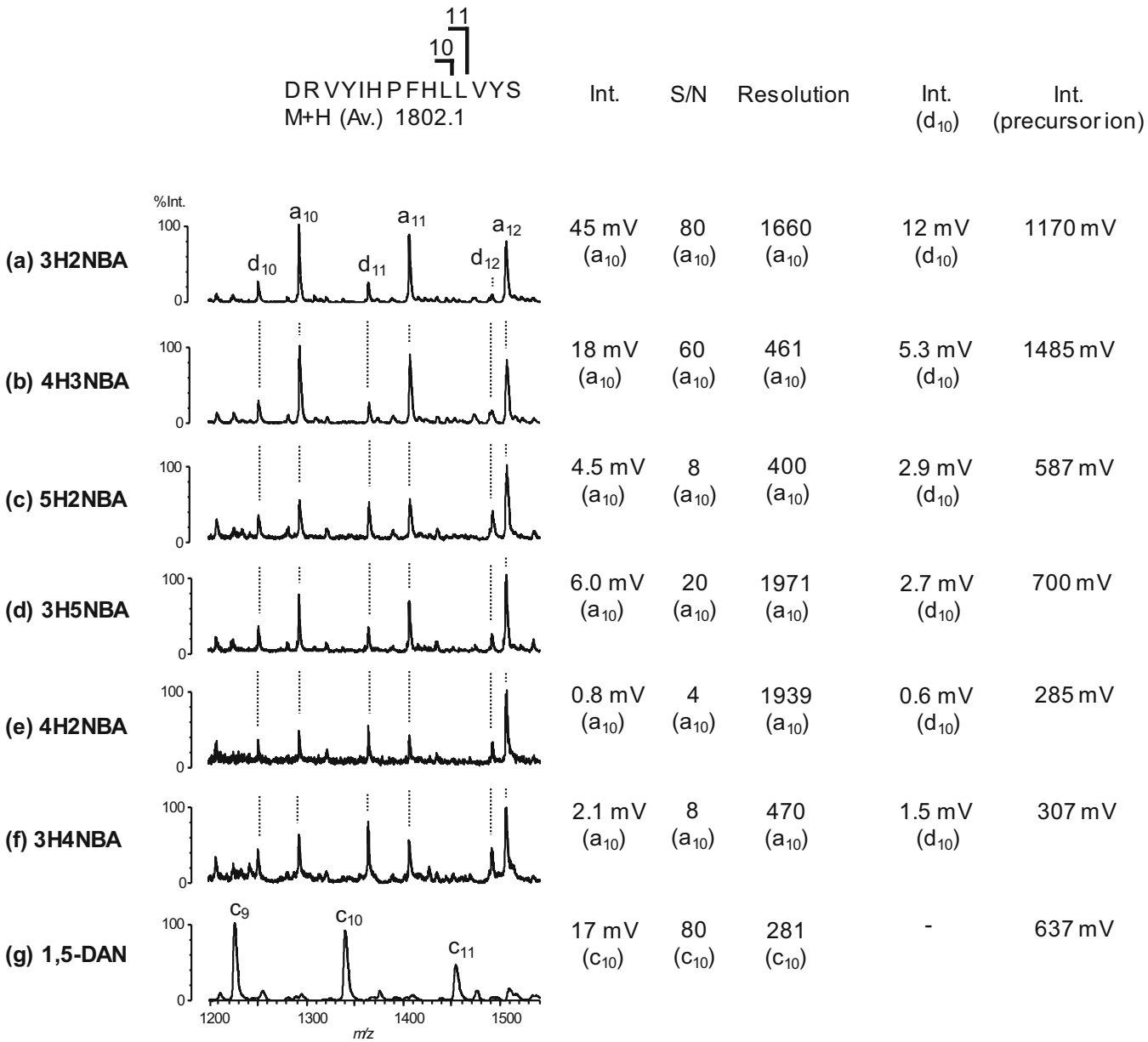

Figure 2. ISD spectra of *N*-acetyl renin substrate at *m/z* 1200–1600 using (**a**) 3H2NBA, (**b**) 4H3NBA, (**c**) 5H2NBA, (**d**) 3H5NBA, (**e**) 4H2NBA, (**f**) 3H4NBA, and (**g**) 1,5-DAN as matrices in linear positive-ion mode. Intensity, S/N ratio and resolution of the representative ion peaks (a_{10}- and c_{10}-ion peaks), and intensity of the precursor ion ($[M + H]^+$) and the d_{10}-ion are also indicated

< 1,5-DAN < 3H2NBA. As a result, the *a*-series ions yield was higher using 3H2NBA or 4H3NBA compared with 3H4NBA, and also higher using 3H2NBA than 1,5-DAN. Moreover, peak intensity of the d_{10}-ion was higher in the following order: 4H2NBA < 3H4NBA < 3H5NBA < 5H2NBA < 4H3NBA < 3H2NBA. It was almost the same with the order of the *a*-series ions yield and the peak intensity of *a*-series ions and the precursor ion. On the other hand, relative ratio of the d_{10}-ion for the a_{10}-ion was as follows: 3H2NBA < 4H3NBA < 3H5NBA < 5H2NBA < 3H4NBA < 4H2NBA. It was almost the reverse of the order of the *a*-series ions yield and the peak intensity of the precursor ion, and *a*- and *d*-series ions. The fact is explained from a mechanism reported by Asakawa et al., in which *a*- and *d*-series ions are possible to be formed from $a^\bullet$ radicals [22]. After preferential generation of *a*-series ions from $a^\bullet$ radicals, *d*-series ions might be limited to form from the $a^\bullet$ radicals. According to Asakawa et al., a high *d*-series ions yield is attributed to a low collision rate [22]. In Figure 2, collision rate might be higher using 3H2NBA than the other isomers. At list, herein, it was confirmed that 3H2NBA was effective for highly sensitive detection of *a*- and *d*-series ions due to the high ionization efficiency of the precursor ion and the high *a*-series ions yield from the precursor ion.

Figure 3 indicates ISD spectra of angiotensin I using 3H2NBA, 4H3NBA, 5H2NBA, 3H5NBA, 4H2NBA, 3H4NBA, and 1,5-DAN as matrices. Intensity, S/N ratio and

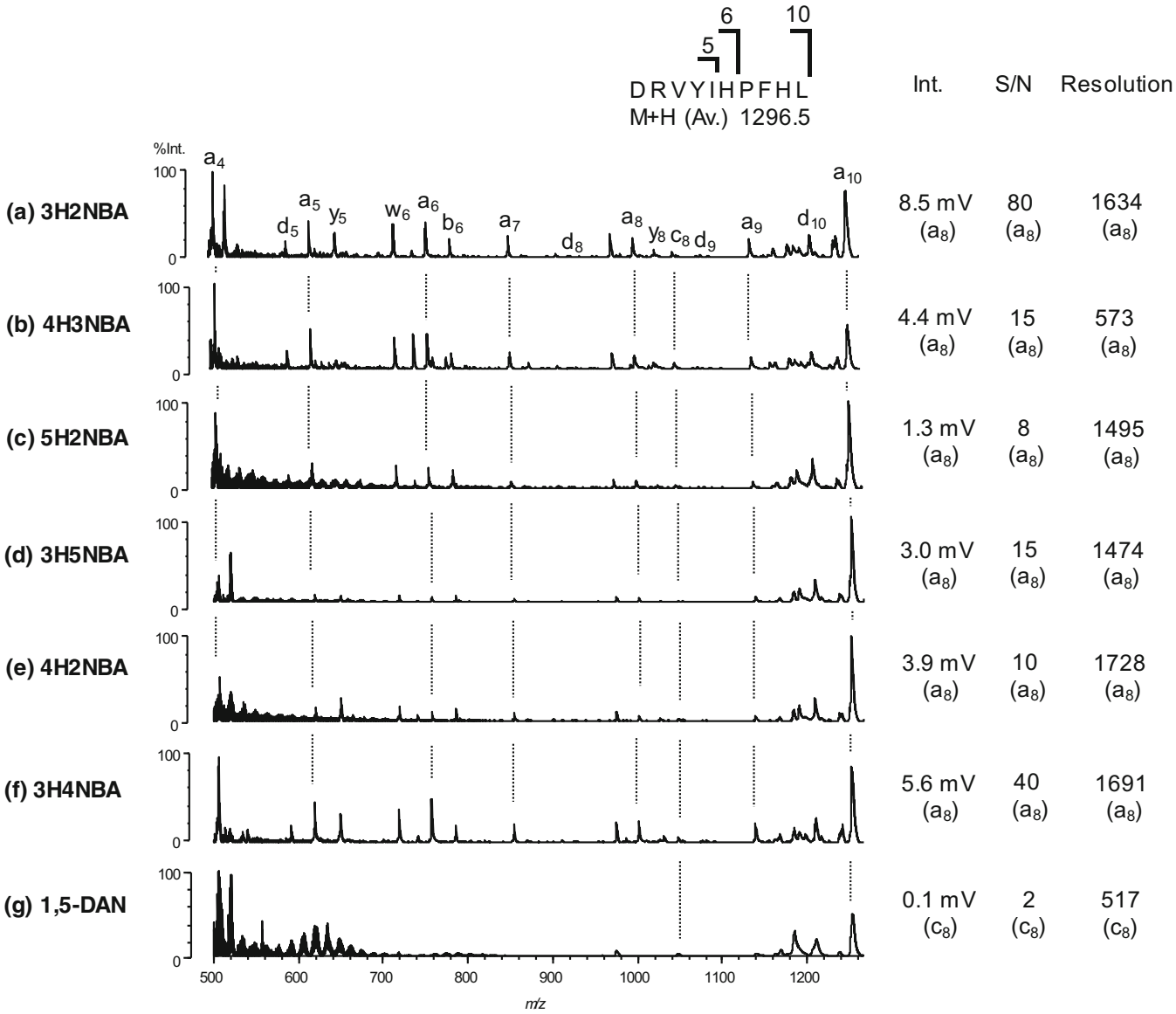

Figure 3. ISD spectra of angiotensin I at *m/z* 500–1265 using (**a**) 3H2NBA, (**b**) 4H3NBA, (**c**) 5H2NBA, (**d**) 3H5NBA, (**e**) 4H2NBA, (**f**) 3H4NBA, and (**g**) 1,5-DAN as matrices with the same laser power in linear positive-ion mode. Intensity, S/N ratio, and resolution of the representative ion peaks (a_8- and c_8-ion peaks) are also indicated

resolution of the representative ion peaks (a_8- and c_8-ion peaks) are also indicated. Amino acid sequence of angiotensin I is similar to that of *N*-acetyl renin substrate shown in Figure 2. Thus, as expected, peak intensity of *a*-series ions was improved using 3H2NBA compared with 3H4NBA and other isomers. But, the difference between 3H2NBA and 3H4NBA was smaller than in Figure 2. In addition, a few *c*-series ions only were detected using 1,5-DAN although a lot of *c*-series ions were detected with sufficient sensitivity in Figure 2 and Figure S1. Remarkable point to note is that the effect of the matrices for ISD depends on amino acid sequence of the analyte even if it is a slight difference. At list, 3H2NBA still demonstrated superior performance for intensity, S/N ratio, and resolution of ISD fragment ions as well or better compared with 3H4NBA and 1,5-DAN.

ISD Analyses Using 3H2NBA

Figure 4 presents ISD spectra of amyloid β 1–16 using 3H2NBA, 4H3NBA, and 3H4NBA. Intensity and resolution of the representative ion peaks (a_{11}-, a_{12}-, and a_{13}-ion peaks) are also indicated. Overall view of the spectra in Figure 4 was presented in Supplemental Information (Figure S2). A lot of *a*- and *x*-series ions were detected using the three matrices. Peak intensity of the a_{12}-ion was higher using 3H2NBA or 4H3NBA compared with 3H4NBA (Figure 4). Peak resolution of a_{11}- and a_{13}-ions was higher using 3H2NBA compared with 4H3NBA or 3H4NBA. As a result, a_{13}- and x_{12}-ions were distinguished using 3H2NBA only (Figure 4a), whereas they were difficult for using 4H3NBA or 3H4NBA (Figure 4b, c). The same tendency of the peak resolution was

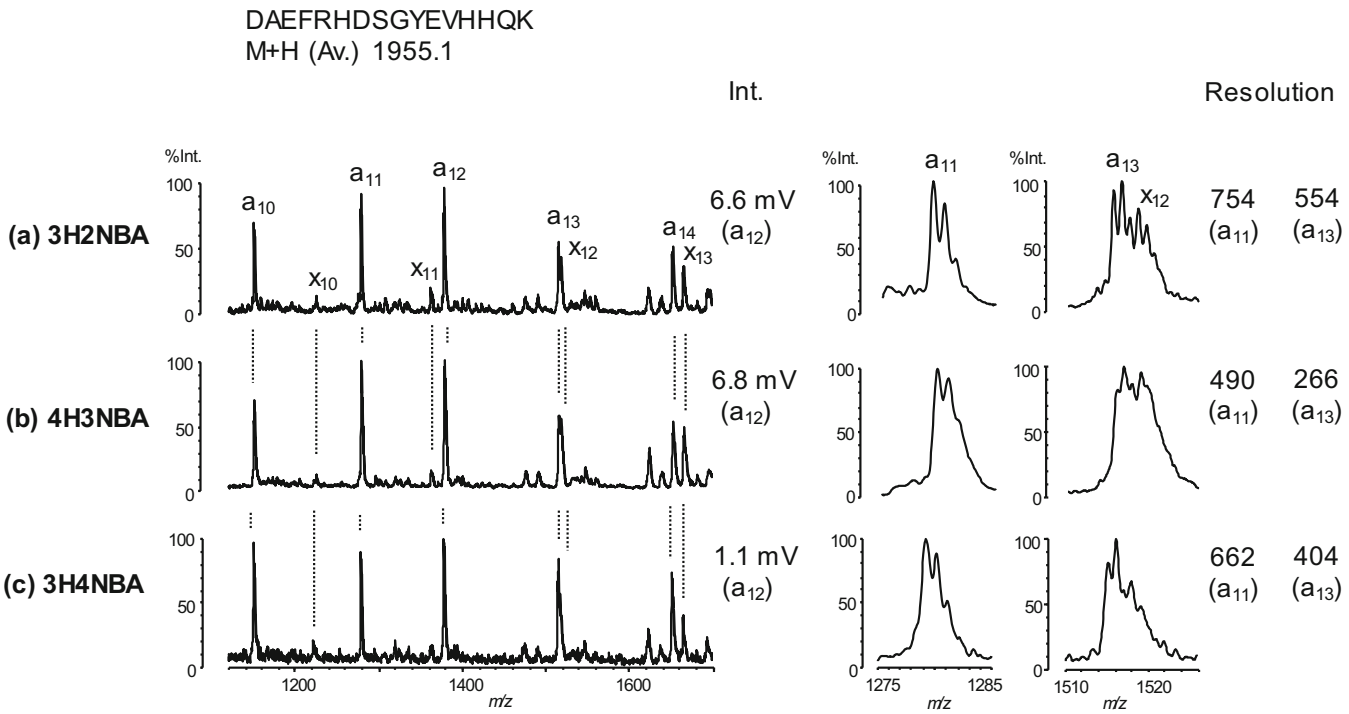

Figure 4. ISD spectra of amyloid β 1–16 at *m/z* 1120–1700 (left) and the extended figures of a_{11}-, a_{13}- and x_{12}-ion peaks (right) using (**a**) 3H2NBA, (**b**) 4H3NBA, and (**c**) 3H4NBA as matrices in linear positive-ion mode. Intensity and resolution of the representative ion peaks (a_{11}-, a_{12}-, and a_{13}-ion peaks) are also indicated

confirmed for other fragment ion peaks. These results indicate that peak intensity and peak resolution of the ISD fragment ions were improved using 3H2NBA compared with 3H4NBA, and the peak resolution was higher using 3H2NBA than 4H3NBA.

Figure 5 shows ISD spectra of amyloid β 1–40 using 3H2NBA, 4H3NBA, and 1,5-DAN. Intensity, S/N ratio, and resolution of the representative ion peaks (a_{15}-, a_{27}-, c_{15}-, and c_{27}-ion peaks) are also indicated. Vertical axes of the spectra were indicated by a scale of millivolts instead of relative intensity (%) due to extremely high intensity of the c_{18}-ion. A lot of *a*- and *d*-series ions were detected using 3H2NBA and 4H3NBA (Figure 5a, b), and *c*-series ions were detected using 1,5-DAN (Figure 5c). The two Leu and two Ile of amyloid β 1–40 were identified by the *d*-series ions (d_{17}-, d_{31}-, d_{32}-, and d_{34}-ions) using 3H2NBA and 4H3NBA (Figure 5a, b). The *d*-series ions effectively distinguished Leu from Ile as described above, whereas they were difficult for using 1,5-DAN. The peak intensity and S/N ratio of the representative ISD fragment ions (a_{15}-, a_{27}-, c_{15}-, and c_{27}-ions) were almost the same using 3H2NBA, 4H3NBA, and 1,5-DAN (Figure 5). Peak resolution of the representative fragment ions using 3H2NBA was slightly higher than using 4H3NBA and 1,5-DAN (Figure 5). The same tendency of the peak resolution was denoted for other fragment ion peaks. These results indicate that peak resolution was improved using 3H2NBA compared with 1,5-DAN, and the peak intensity and S/N ratio were similar for them.

Figure 6 presents ISD spectra of ACTH 18–39 using 3H2NBA, 4H3NBA, 3H4NBA, and 1,5-DAN. Intensity, S/N ratio, and resolution of the representative ion peaks (a_{16}- and c_{16}-ion peaks), and intensity of the precursor ion ($[M + H]^+$) are also indicated. A lot of *a*- and *d*-series ions were detected using 3H2NBA, 4H3NBA, and 3H4NBA (Figure 6a–c), and *c*-series ions were detected using 1,5-DAN (Figure 6c). The a_6-ion and a_{18}-ion were detected even at the N-terminal side of Pro using 3H2NBA and the isomers, whereas the sequencing is difficult to achieve for *c*-series ions using 1,5-DAN. However, in this case, the peak intensity and S/N ratio of the representative ISD fragment ion peaks were lower using 3H2NBA compared with 3H4NBA. This result is probably an example that the effect of matrices for ISD depends on the analyte. Intensity of the precursor ion was higher in the following order: 3H2NBA < 4H3NBA < 3H4NBA < 1,5-DAN. The order is the same with the order of the intensity of the a_{16}-ion (or the c_{16}-ion). The intensity of the precursor ion is influenced by the affinity of the matrix for the analyte. ISD fragment ions are produced from the precursor ion. Thus, the intensity of the ISD fragment ions was probably influenced by the affinity of the matrix for the analyte in detection of the precursor ion.

From the evaluation of the isomers described above, it was concluded that 3H2NBA is one of the most effective oxidizing matrices for ISD due to higher peak intensity, S/N ratio, and peak resolution. The effect of the matrix is somewhat influenced by the affinity of the matrix for the analytes, but 3H2NBA is still important to have high potential as an oxidizing matrix for ISD.

Figure 1B presents photo images of a matrix/analyte dried spot on a MALDI sample plate using 3H2NBA, 4H3NBA, and

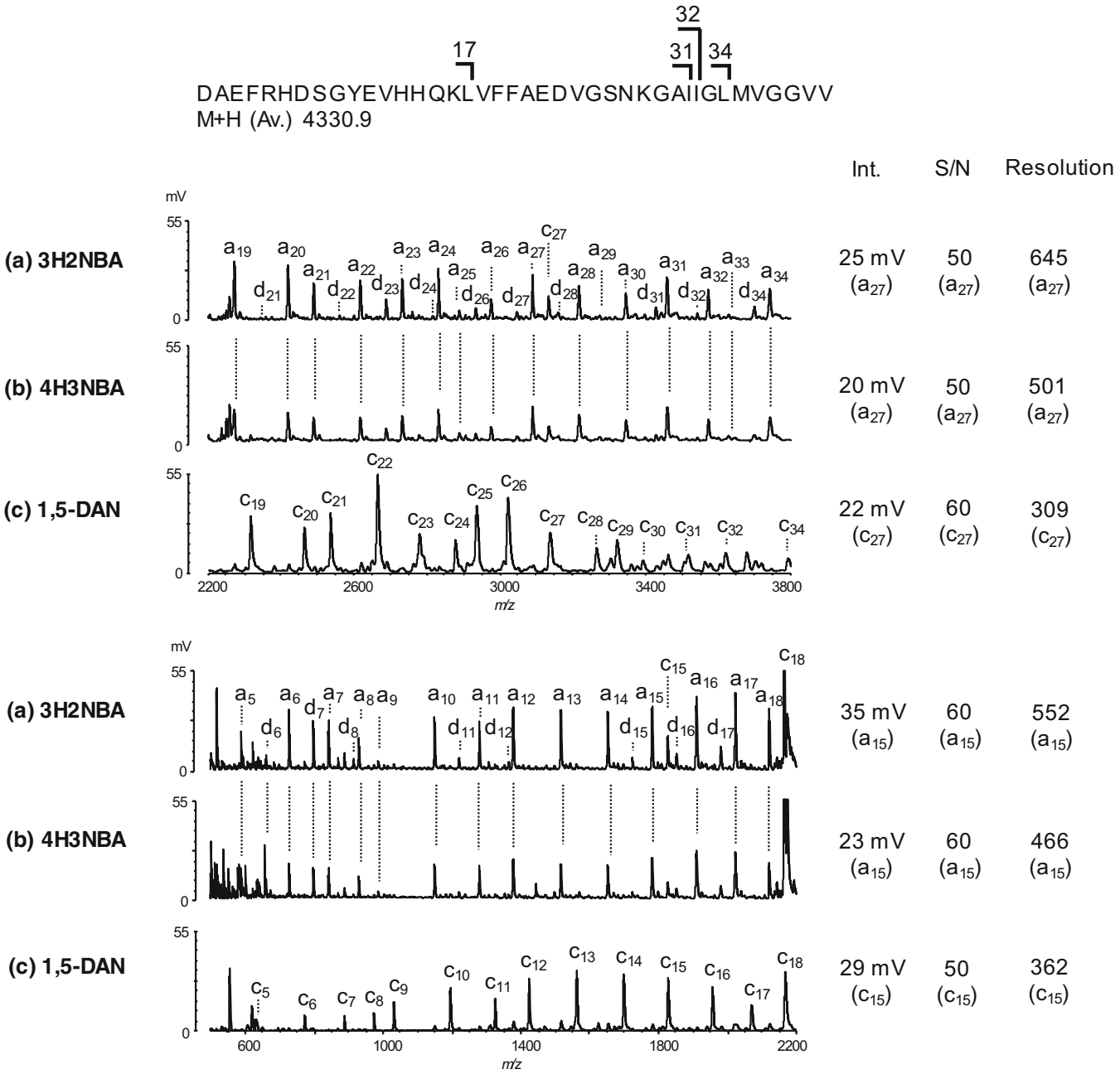

Figure 5. ISD spectra of amyloid β 1–40 using (**a**) 3H2NBA, (**b**) 4H3NBA, (**c**) 3H4NBA, and (**d**) 1,5-DAN as matrices in linear positive-ion mode. Intensity, S/N ratio, and resolution of the representative ion peaks (a_{15}-, a_{27}-, c_{15}-, and c_{27}-ion peaks) are also indicated

1,5-DAN. The dried spot using 1,5-DAN was a large needle crystal that was comparatively thick and inhomogeneous (Figure 1Bc). In fact, the ions were detected partially limited "sweet spots" on a dried spot using 1,5-DAN. On the other hand, the spot was a relatively homogeneous thin layer using 3H2NBA (Figure 1Ba) and a densely distributed relatively homogeneous thin layer using 4H3NBA (Figure 1Bb). Generally, thin homogeneous crystallization has been known to achieve high-resolution analyses in MALDI TOFMS. Probably, thus, the ions were detected with higher peak resolution from the spot using 3H2NBA or 4H3NBA compared with 1,5-DAN as shown in Figures 2, 5, and 6. Additionally, the ions were detected from the entire area of a matrix/analyte spot. The property of 3H2NBA or 4H3NBA is the same with 3H4NBA described in a previous report [31]. In Figure 4, peak resolution of *a*-series ions was higher using 3H2NBA than 4H3NBA. The fact can be explained by the difference of thickness of a matrix/analyte dried spot using 3H2NBA and 4H3NBA, in which the crystal was more thin layer using 3H2NBA than 4H3NBA (Figure 1Ba, Bb).

For the issues (i)–(vi) of 1,5-DAN referred to in "Introduction" section, the following three issues were solved by 3H2NBA for several peptides as described above: (i) 3H2NBA as a reducing matrix generated *a*-series ions even at

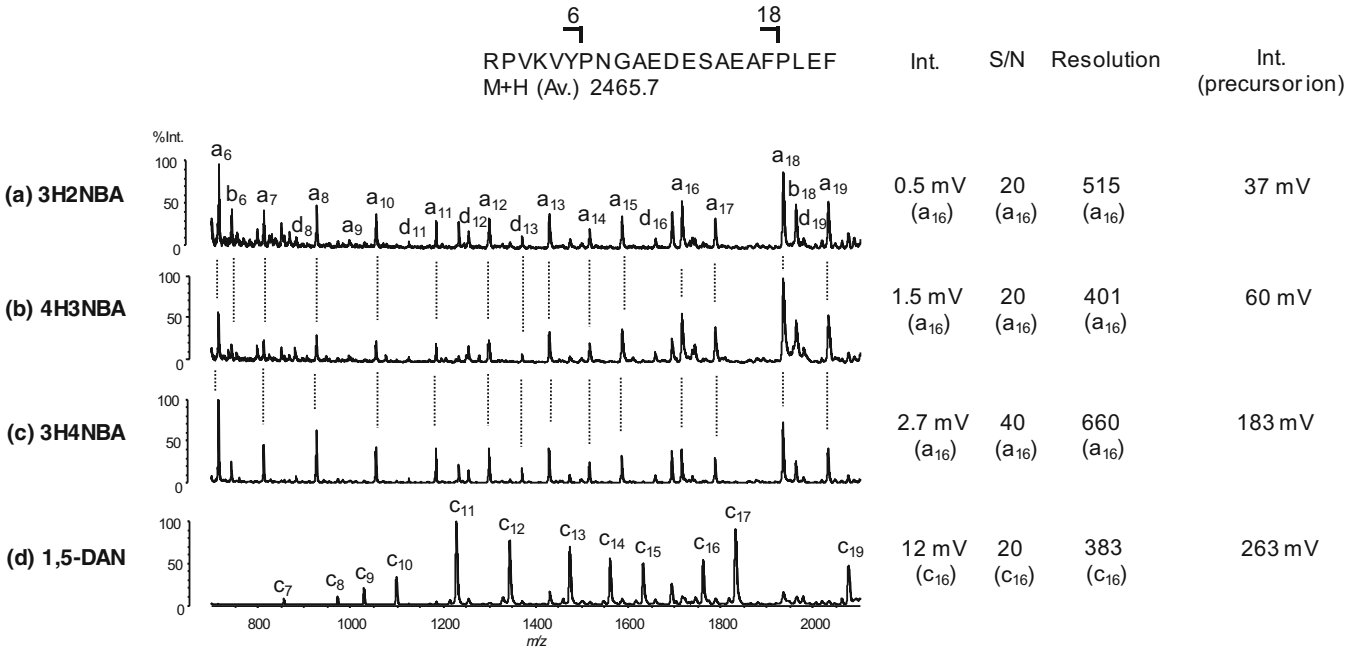

Figure 6. ISD spectra of adrenocorticotropic hormone fragment 18–39 (ACTH 18–39) at *m/z* 700–2100 using (**a**) 3H2NBA, (**b**) 4H3NBA, (**c**) 3H4NBA, and (**d**) 1,5-DAN as matrices with the same laser power in linear positive-ion mode. Intensity, S/N ratio and resolution of the representative ion peaks (a_{16}- and c_{16}-ion peaks), and intensity of the precursor ion ($[M + H]^+$) are also indicated

the left side of Pro (Figures 3 and 6, and Figure S1). (ii) 3H2NBA enabled to distinguish Leu and Ile by *d*-series ions (Figures 2, 3 and 5, and Figure S1). (iii) Relatively homogeneous thin matrix/analyte crystallization was observed using 3H2NBA leading to higher peak resolution and rapid measurement due to no need to find "sweet spots" (Figure 1B). In addition, other three issues of 1,5-DAN were evaluated for 3H2NBA as follows: (iv) Sublimation of 3H2NBA was slower as reported for 3H4NBA [31], resulting to higher reproducibility and long-time measurement. (v) Stability of 3H2NBA in solution was higher as reported for 3H4NBA [31] in which ISD fragment ions were detected with approximately the same intensity using both matrix solution prepared on the day and 4 months ago. (vi) Toxicity including carcinogenicity of 3H2NBA has not been reported. Thus, all the issues (i)–(vi) of 1,5-DAN were solved using 3H2NBA, just as reported for 3H4NBA [31]. Added to this, 3H2NBA indicated almost the same or higher peak intensity of the ISD fragment ions compared with 1,5-DAN. Furthermore, it is significant that the effect of 3H2NBA depends on the analytes; that is, it is influenced by the amino acid sequence of the analyte and the affinity of the matrix for the analyte.

Chemical Structure of 3H2NBA for Cα–C Bond Cleavage

It was confirmed that peak intensity of *a*-series ions was improved using 3H2NBA and 4H3NBA compared with 3H4NBA for several peptides (Figures 2 and 4). Especially, the intensity was almost the same or higher for *a*-series ions using 3H2NBA compared with *c*-series ions using 1,5-DAN (Figures 2, 3, and 5). In this case, the difference of the effect of the matrices can be considered from the difference of the matrix structure. The difference of chemical structure of 3H2NBA and 4H3NBA from 3H4NBA is just a position of a NO_2 group and a OH group on a benzene ring. NO_2 groups have been reported to work as hydrogen acceptors [20, 23, 32]. OH groups have been reported to work as hydrogen donors [16, 17, 23, 33]. According to Asakawa et al., a NO_2 group on 5-NSA (2H5NBA) has high affinity for NH groups from the amide portion of peptide backbone and accepts hydrogen from NH groups, providing *a*- and *x*-series ions [23]. According to Brown et al., OH groups on a matrix form hydrogen bonds with basic sites of the analytes and then contribute to an exothermic proton transfer [13, 14, 16]. In the previous report, positionally nearby relation of a OH group and a NO_2 group like a "3,4-relation" of 3H4NBA is effective for highly sensitive detection of *a*- and *d*-series ions [31]. In this study, a "3,2-relation" or a "4,3-relation" of 3H2NBA or 4H3NBA was effective for improvement of the intensity of *a*-series ions compared with a "3,4-relation" of 3H4NBA. In this case, a positional relation of a NO_2 group located between a OH group and a COOH group on a benzene ring was effective for the intensity improvement. The COOH group acts as strong hydrogen donors and also acceptors; thus, the COOH group can form an intramolecular hydrogen bond with a NO_2 group as hydrogen acceptors. Simultaneously, the NO_2 group can form another intramolecular hydrogen bond with a OH group nearby located on a benzene ring. Both hydrogen bonds contribute to an exothermic proton transfer leading to intensity improvement. On the other hand, in a "3,4-relation" of 3H4NBA, it is difficult to form intramolecular hydrogen bonds between a COOH group and a OH group or a NO_2 group compared with

the case of 3H2NBA or 4H3NBA because a NO_2 group can form more strong hydrogen groups than a OH group. Thus, 3H2NBA or 4H3NBA enables to generate *a*- and *d*-series ions with higher intensity compared with 3H4NBA. The intramolecular hydrogen bonds were generally formed more strongly at the nearby position on a benzene ring. It leads to a hypothesis that 3H2NBA has potential to detect the fragment ions with higher intensity than 4H3NBA, as demonstrated in Figures 2 and 5. That is, 3H2NBA pulls out hydrogen from NH groups of peptide backbone to detect *a*- and *x*-series ions with higher intensity, probably due to lower electrical charge (or electron density) on the NO_2 group and strong ionization property based on the structure compared with other isomers.

Table S1 indicates the charge (Hückel) on the nitrogen atom of the NO_2 group for 3H2NBA and the isomers. The charge was higher in the following order: 3H2NBA < 4H2NBA < 5H2NBA < 2H6NBA < 3H4NBA < 4H3NBA < 2H3NBA < 2H5NBA < 2H4NBA < 3H5NBA. Generally, it is known that matrices with lower charge readily generate NO_2 radicals. The NO_2 radicals result in a Cα–C bond cleavage. Thus, 3H2NBA has a potential to more effectively produce *a*- and *d*-series ions than 3H4NBA and 4H3NBA.

Figure S3 indicates mass spectra of amyloid *β* 1–16 using 3H2NBA, 4H3NBA, and 3H4NBA, possessing an OH group, and 3,4-DNBA not possessing an OH group. As a result, peak intensity of the protonated intact molecule ($[M + H]^+$) was extremely lower using 3,4-DNBA compared with other three matrices. The fact suggests that the OH group contributes to ionization of the intact molecule. In addition, the protonated intact molecule was detected with higher intensity using 3H2NBA and 4H3NBA than 3H4NBA (Figure S3). It means that a positional relation of a NO_2 group located between an OH group and a COOH group on a benzene ring leads to highly sensitive detection of the protonated intact molecule. That is, the OH group is necessary for ionization of the intact molecule, and the positional relation of the NO_2 group is effective for highly sensitive detection of the protonated intact molecule. In Figure S3, the highest intensity was confirmed using 4H3NBA. It corresponds to the result of Figure 2. The facts can be explained by the results of UV absorbance described before, in which it was higher for 4H3NBA and 3H2NBA than 3H4NBA, and 4H3NBA showed highest absorbance (data not shown). Typically, intensity of *a*-series ions should be explained by both the ionization efficiency of the precursor ion and the *a*-series ions yield from the precursor ion. The *a*-series ions yield was higher using 3H2NBA or 4H3NBA than 3H4NBA, and furthermore 3H2NBA than 4H3NBA and 1,5-DAN, as described before. In actual, after UV laser irradiation, 3H2NBA and the isomers are absorbed and excited, and then proceed exothermic reaction such as proton transfer and fragmentation to ionize intact molecules and produce *a*- and *d*-series ions. The reactions proceed based on each matrix structure. Eventually, it was concluded that 3H2NBA and 4H3NBA in both the former and the later reaction, especially 3H2NBA in the later reaction and totally, have more potential for highly sensitive detection of *a*- and *d*-series ions compared with 3H4NBA and 1,5-DAN.

In 3H2NBA structure, a NO_2 group located between a OH group and a COOH group on a benzene ring was considered to cause the improvement of peak intensity of ISD fragment ions and simultaneously have high affinity for NH groups from the amide portion of peptide backbone to provide *a*-series ions. Thus, 3H2NBA is a matrix to be able to effectively pull out a hydrogen from the peptide backbone. Positional relation of an OH group and a NO_2 group on 3H2NBA structure was probably in an almost perfect balance, that is, a lower electrical charge (or electron density) of the NO_2 group, to make effectively progress the Cα–C bond cleavage and ionization.

For highly sensitive detection of ISD fragments using 3H2NBA by taking account of the characteristics, highly sensitive detection of the precursor ion was needed as a premise. For the highly sensitive detection of the precursor ions, the matrix needs a high affinity for the analyte. One of the subjects for a further study of ISD seems to establish a method which is effective for any analytes.

Conclusions

3H2NBA was reported as a novel oxidizing matrix for ISD. It provides *a*- and *d*-series ions with higher peak intensity and peak resolution for several peptides. The *d*-series ions enable to distinguish Leu and Ile, and the *a*-series ions were provided even at the N-terminal side of Pro. Peak intensity of the ISD fragment ions was higher using 3H2NBA than the other isomers, and almost the same or higher compared with 1,5-DAN for *N*-acetyl renin substrate, angiotensin I, amyloid *β* 1–16, and amyloid *β* 1–40. In several cases, peak resolution of the fragment ions was clearly higher using 3H2NBA compared with 1,5-DAN. The matrix/analyte dried spot is relatively thin and homogeneous. As a result, 3H2NBA solved all the issues of 1,5-DAN for several peptides. Remarkable point is that the effects of 3H2NBA are somewhat influenced by the analyte. For example, *a*-series ions of ACTH 18–39 were detected higher intensity using 3H4NBA than 3H2NBA probably due to the poor affinity of 3H2NBA for the analyte. In the future, ISD method is required to be effective for all kind of analytes. Between now and then, 3H2NBA is expected to contribute the ISD analyses as a single matrix as one of the most effective oxidizing matrices or in combination with the results using 1,5-DAN.

References

1. Karas, M., Bachmann, D., Hillenkamp, F.: Influence of the wavelength in high-irradiance ultraviolet laser desorption mass spectrometry of organic molecules. Anal. Chem. **57**, 2935–2939 (1985)
2. Karas, M., Bachmann, D., Bahr, U., Hillenkamp, F.: Matrix-assisted ultraviolet laser desorption of non-volatile compounds. Int. J. Mass Spectrom. Ion Process. **78**, 53–68 (1987)
3. Tanaka, K., Waki, H., Ido, Y., Akita, S., Yoshida, Y., Yoshida, T.: Protein and polymer analyses up to *m/z* 100000 by laser ionization time-of-flight mass spectrometry. Rapid Commun. Mass Spectrom. **2**, 151–153 (1988)

4. Karas, M., Hillenkamp, F.: Laser desorption ionization of proteins with molecular masses exceeding 10000 daltons. Anal. Chem. **60**, 2299–2301 (1988)
5. Fenn, J.B., Mann, M., Meng, C.K., Wong, S.F., Whitehouse, C.M.: Electrospray ionization for mass spectrometry of large biomolecules. Science. **246**, 64–71 (1989)
6. Biemann, K.: Sequencing of peptides by tandem mass spectrometry and high-energy collision-induced dissociation. Methods Enzymol. **193**, 455–479 (1990)
7. Kaufmann, R., Kirsch, D., Spengler, B.: Sequencing of peptides in a time-of-flight mass spectrometer: evaluation of postsource decay following matrix-assisted laser desorption ionization (MALDI). Int. J. Mass Spectrom. Ion Process. **131**, 355–385 (1994)
8. Brown, R.S., Lennon, J.J.: Sequence-specific fragmentation of matrix-assisted laser-desorbed protein/peptide ions. Anal. Chem. **67**, 3990–3999 (1995)
9. Reiber, D.C., Grover, T.A., Brown, R.S.: Identifying proteins using matrix-assisted laser desorption/ionization in-source fragmentation data combined with database searching. Anal. Chem. **70**, 673–683 (1998)
10. Demeure, K., Quinton, L., Gabelica, V., De Pauw, E.: Rational selection of the optimum MALDI matrix for top-down proteomics by in-source decay. Anal. Chem. **79**, 8678–8685 (2007)
11. Asakawa, D.: Principles of hydrogen radical mediated peptide/protein fragmentation during matrix-assisted laser desorption/ionization mass spectrometry. Mass Spectrom. Rev. **35**, 535–556 (2016)
12. Hardouin, J.: Protein sequence information by matrix-assisted laser desorption/ionization in-source decay mass spectrometry. Mass Spectrom. Rev. **26**, 672–682 (2007)
13. Brown, R.S., Carr, B.L., Lennon, J.J.: Factors that influence the observed fast fragmentation of peptides in matrix-assisted laser desorption. J. Am. Soc. Mass Spectrom. **7**, 225–232 (1996)
14. Brown, R.S., Feng, J., Reiber, D.C.: Further studies of in-source fragmentation of peptides in matrix-assisted laser desorption-ionization. Int. J. Mass Spectrom. Ion Process. **169**(/170), 1–18 (1997)
15. Takayama, M., Tsugita, A.: Does in-source decay occur independent of the ionization process in matrix-assisted laser desorption? Int. J. Mass Spectrom. **181**, L1–L6 (1998)
16. Takayama, M.: In-source decay characteristics of peptides in matrix-assisted laser desorption/ionization time-of-flight mass spectrometry. J. Am. Soc. Mass Spectrom. **12**, 420–427 (2001)
17. Sakakura, M., Takayama, M.: In-source decay and fragmentation characteristics of peptides using 5-aminosalicylic acid as a matrix in matrix-assisted laser desorption/ionization mass spectrometry. J. Am. Soc. Mass Spectrom. **21**, 979–988 (2010)
18. Osaka, I., Sakai, M., Takayama, M.: 5-Amino-1-naphthol, a novel 1,5-naphthalene derivative matrix suitable for matrix-assisted laser desorption/ionization in-source decay of phosphorylated peptides. Rapid Commun. Mass Spectrom. **27**, 103–108 (2013)
19. Smargiassso, N., Quinton, L., De Pauw, E.: 2-Aminobenzamide and 2-aminobenzoic acid as new MALDI matrices inducing radical mediated in-source decay of peptides and proteins. J. Am. Soc. Mass Spectrom. **23**, 469–474 (2012)
20. Asakawa, D., Takayama, M.: Cα-C bond cleavage of the peptide backbone in MALDI in-source decay using salicylic acid derivative matrices. J. Am. Soc. Mass Spectrom. **22**, 1224–1233 (2011)
21. Asakawa, D., Sakakura, M., Takayama, M.: Influence of initial velocity of analyte on in-source decay products in MALDI mass spectrometry using salicylic acid derivative matrices. Int. J. Mass Spectrom. **337**, 29–33 (2013)
22. Asakawa, D., Takayama, M.: Fragmentation process of hydrogen-deficient peptide radicals in matrix-assisted laser desorption/ionization in-source decay mass spectrometry. J. Phys. Chem. B. **116**, 4016–4023 (2012)
23. Asakawa, D., Sakakura, M., Takayama, M.: Matrix effect on in-source decay products of peptides in matrix-assisted laser desorption/ionization. Mass Spectrometry. **1**, A0002 (2012)
24. Quinton, L., Demeure, K., Dobson, R., Gilles, N., Gabelica, V., De Pauw, E.: New method for characterizing highly disulfide-bridged peptides in complex mixtures: application to toxin identification from crude venoms. J. Proteome Res. **6**, 3216–3223 (2007)
25. Demeure, K., Gabelica, V., De Pauw, E.A.: New advances in the understanding of the in-source decay fragmentation of peptides in MALDI-TOF-MS. J. Am. Soc. Mass Spectrom. **21**, 1906–1917 (2010)
26. Debois, D., Bertrand, V., Quinton, L., De Pauw-Gillet, M.-C., De Pauw, E.: MALDI-in source decay applied to mass spectrometry imaging: a new tool for protein identification. Anal. Chem. **82**, 4036–4045 (2010)
27. Calligaris, D., Longuespée, R., Debois, D., Asakawa, D., Turtoi, A., Castronovo, V., Noél, A., Bertrand, V., De Pauw-Gillet, M.-C., De Pauw, E.: Selected protein monitoring in histological sections by targeted MALDI-FTICR in-source decay imaging. Anal. Chem. **85**, 2117–2126 (2013)
28. Lemaire, P., Debois, D., Smargiasso, N., Quinton, L., Gabelica, V., De Pauw, E.A.: Use of 1,5-diaminonaphthalene to combine matrix-assisted laser desorption/ionization in-source decay fragmentation with hydrogen/deuterium exchange. Rapid Commun. Mass Spectrom. **27**, 1837–1846 (2013)
29. Asakawa, D., Calligaris, D., Zimmerman, T.A., De Pauw, E.: In-source decay during matrix-assisted laser desorption/ionization combined with the collisional process in an FTICR mass spectrometer. Anal. Chem. **85**, 7809–7817 (2013)
30. In: Bioassay of 1,5-Naphthalenediamine for Possible Carcinogenicity, National Cancer Institute Carcinogenesis Technical Report Series, No. 143, U.S. Department of Health, Education, and Welfare (DHEW) Public Health Service: National Institutes of Health, Maryland (1978)
31. Fukuyama, Y., Izumi, S., Tanaka, K.: 3-Hydroxy-4-nitrobenzoic acid as a MALDI matrix for in-source decay. Anal. Chem. **88**, 8058–8063 (2016)
32. Morrison, H., Migdalof, B.H.: Photochemical hydrogen abstraction by the nitro group. J. Org. Chem. **30**, 3996–3996 (1965)
33. Takayama, M.: N-Cα bond cleavage of the peptide backbone via hydrogen abstraction. J. Am. Soc. Mass Spectrom. **12**, 1044–1049 (2001)